ELSEVIER

Cement and Concrete Composites **19** (1997) 149–160
Published by Elsevier Science Ltd
Printed in Great Britain. All rights reserved
0958-9465/97/$17.00

PII:S0958-9465(97)00005-X

The Effects of Confinement on the Failure Orientation in Cementitious Materials Experimental Observations

Craig A. Rutland[a] & Ming L. Wang[b]

[a]21st Civil Engineer Squadron, Peterson AFB, CO 80914-2370, USA
[b]Department of Civil Engineering, University of New Mexico, Albuquerque, NM, USA

(Received 20 February 1996; accepted 3 January 1997)

Abstract

The literature is replete with studies of cementitious and geologic materials under multiaxial states of stress. However, there still exists division over the character of the failure mode under multiaxial states of stress. Some experts state that the failure is diffuse. The classical barrel-shaped specimen removed from a test cell intact is cited as evidence. Other researchers state that the failure is characterized by failure planes orientated parallel to the maximum compressive stress for all values of hydrostatic pressure. Tests on geologic materials have shown that the failure is nearly parallel to the maximum compressive stress under uniaxial stress. The orientation increases angle with respect to the maximum compressive stress as the confining pressure increases. Other sources simply state that there is a change in mode from splitting failure to crushing failure as confinement increases. The objective of this research is to better define the character of the failure mechanism as confining pressure increases. In this study triaxial tests on 95 mortar cylinders show that there is a change in the orientation of the failure plane as confining pressure is increased. The failure is characterized by a distinct failure surface or surfaces that change orientation from nearly vertical to angled as confinement increases. Furthermore, test data indicate that localized deformations occur within 5% of the peak stress. These results imply that the failure is truly characterized through localized deformations and is not diffuse. Knowledge of such behavior is important because it places restrictions on the form of the constitutive model in order to predict these features. The implications of these findings on the constitutive model are discussed in detail in a companion paper. Published by Elsevier Science Ltd.

Keywords: Multiaxial stress, mortar, failure mechanism, damage, failure plane, confining stress, modelling.

INTRODUCTION

Triaxial tests performed by Wawersik and Brace[1] and Murrell[2] on rocks have shown that the angle of the failure plane for geologic materials changes with increasing confining pressure. At present there is no data for concrete that relates the confinement to the change in the angle of the principal failure plane. However, Palaniswamy and Shah,[3,4] commenting on triaxial tests on cement paste, mortar and concrete, state that two distinct modes of behavior were observed. Specifically, a splitting failure at low confining pressures and a crushing failure at large confining pressures.

On the other hand, Zimmerman and Traina[5] state that the failure plane is always orientated parallel to the direction of maximum compressive stress. The apparatus used in the tests by these authors employed platens to apply lateral pressure to the specimens. These platens may have constrained the true failure modes of the specimens. Tests by Gerstle *et al.*[6] using several different loading devices showed that boundary constraints from the use of platens for lateral loading inhibit transverse deformations.

In this study it is shown that there is a change in the orientation of the failure plane as confining pressure increases. It is observed that it is essential to relieve friction between the platens, since this friction severely affects the development of the failure mechanism and consequently its orientation. It is also found that localized behavior begins within 5% of the peak stress. Knowledge of such behavior is important because it places restrictions on the constitutive model, just as the laws of thermodynamics do.

EXPERIMENTAL TECHNIQUE

Triaxial tests were performed with confining pressures ranging from 0 to 56 MPa (8000 psi). A total of 95 cylinders were tested in uniaxial or triaxial compression. An essential part of this study was to evaluate how the method of applying the loads affects the behavior. Specifically, it is necessary to evaluate the effect of the methods used to relieve friction between the load platens and the specimens.

EQUIPMENT SET-UP

A Behavioral Science Engineering Laboratories 70 MPa (10 ksi) triaxial test cell was used to apply the lateral confining pressure. The test cell was placed in a Tinius Olson Super 'L' universal test machine. The test cell had a pressure transducer that was used to monitor fluid pressure inside the cell. The axial load was applied with a universal testing machine.

Strain gauges were used in 56% of the tests. The remaining tests recorded only load–displacement data. Measurements Group, Inc., EA-06-500BL-350 strain gauges were used to measure the strains. Four strain gauges were used on all of the triaxial tests with strain gauges. Two of the gauges were located at the midheight of the specimen. One of the gauges was positioned to measure the axial strain and the other was positioned to measure the circumferential strain. The other two gauges were located near the end of the specimen and were positioned for measuring the axial and circumferential strains. Figure 1 shows one set of gauges placed at the midsection of the specimen. Axial load and displacement data were recorded on an X–Y plotter. Some of the test data were digitized and stored on an IBM-compatible personal computer using an analog to digital converter.

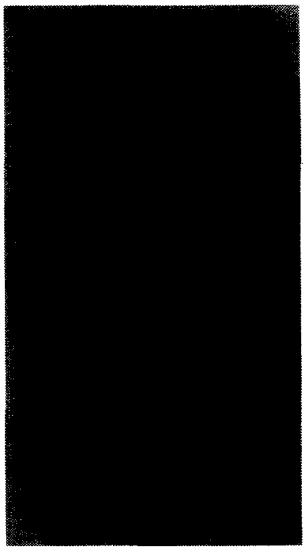

Fig. 1. Gauge placement.

SPECIMEN PREPARATION

All triaxial specimens were prepared with a water/cement ratio between 0.42 and 0.47. The sand was oven dried. The gradation of the aggregates (sand) is given in Table 1. The cement/aggregate ratio was 0.25 by weight. Superplasticizer, Fritz-pak Supercizer 6, was added to increase the workability of the mixes, 0.3% by weight of cement.

Seventy-five specimens measuring 5 cm (2 in) in diameter by 10 cm (4 in) tall were cast in three batches of 25. Twelve specimens 5 cm (2 in) in diameter by 20 cm (8 in) tall were cast in a separate batch. Eight of the 20 cm (8 in) tall specimens were cut in half; the others were cut down to 15 cm (6 in) to fit in to the test cell.

Table 1.

Sand gradation Passing–Retaining Sieve #–Sieve #	*% by weight*
#4–#8	**20.0**
#8–#16	**20.5**
#16–#30	**21.0**
#30–#40	**15.5**
#40–#50	**11.0**
#50–#100	**9.5**
#100–#200	**2.0**
<#200	**0.5**

Eight beams were cast and tested in three point bending to determine the tensile properties of the mix. The beam measured 51 (20) × 3.8 (1.5) × 3.8 cm (1.5 in) and were tested in three point bending. The average modulus of rupture is 7 MPa (1 ksi).

To aid in the relief of the friction between the platens and the specimens, cap blocks were prepared. The cap blocks were 5 cm (2 in) in diameter and 1.3–2.5 cm thick. The mix design for the cap blocks was similar to that of the specimens with the exceptions that the cement/aggregate ratio was increased to 0.4, the water/cement ratio was decreased to 0.35 and the amount of superplasticizer was increased to 0.5%. The objective was to produce a material with similar deformation properties, but with a higher strength. The modulus and lateral extension ratio of the two materials were similar (within 5%) while the uniaxial strength of the cap blocks was 50% larger than the strength of the specimens.

The specimens were stream cured at 60°C for 7–9 days. Most specimens were tested more than 3 weeks after being poured. Nine specimens were tested approximately 2 weeks after being poured. The ends of the 10 cm (4 in) tall cylinders were cut to obtain flat parallel surfaces. All specimens and cap blocks were polished on a lap table containing a coarse grit (100) lap pad. Gauges were applied using Measurements Group, Inc., standard procedures with M-Bond AE-10 adhesive. The cylinders and cap blocks contained air voids on the surfaces which would tear the triaxial membranes. In order to protect the membranes, the surface voids were filled with clay. Triaxial membranes were placed on the specimens.

Several methods of relieving the friction between the specimen and the platens were tested and evaluated using uniaxial tests: no relief, cap blocks alone, cap blocks with grease, cap blocks with grease and polyethylene sheets (PGP pads), grease with polyethylene sheets alone, and rubbers sheets. Ten specimens and four cap block cylinders were tested without any relief of the friction. This was done to determine material properties for comparison to the cap block material and to the other methods. Based on these tests, cap blocks alone, cap blocks with grease and cap blocks with PGP pads were used to relieve the friction.

The design of the grease was obtained from work by Labuz and Bridell.[7] The grease was made by dissolving equal proportions by weight of steric acid into petroleum jelly (Vaseline) at 70°C. Friction reducing pads were made by sandwiching the grease between two 0.1 mm (0.004 in) thick polyethylene sheets. The polyethylene–grease–polyethylene pads are simply referred to as PGP pads. Tests on specimens using the cap blocks and PGP pads required a hose clamp to be placed at each interface of the specimen and the cap block, to prevent slippage. Even with these clamps fastened, the specimens would slip. The amount of slippage increased with increasing confining pressure.

TEST MATRIX

Tests were performed at 0, 1.7, 3.5, 7, 14, 28, 42 and 56 MPa (0, 0.25, 0.5, 1, 2, 4, 6, 8 ksi) using cap blocks, caps w/grease and caps w/PGP pads. Problems with specimen slippage prevented tests at 56 MPa with caps w/PGP pads. Two specimens were tested under hydrostatic compression. The bulk modulus from these tests was 17 GPa (2400 ksi).

The orientation of the failure plane at 3.5 MPa was essentially from one corner (edge) to the opposite. Four tests were performed with the 15 cm (6 in) long specimens with caps alone for relief at 3.5 MPa to preclude the possibility that the end effects might be influencing the results.

The tests were conducted using one of three main load sequences. The first was a standard triaxial loading where the displacement was monotonically increased up to and past the peak load. The second, intermittent cycling, was a standard triaxial loading, but the load was cycled down to the hydrostatic pressure periodically. The third type, intermittent creep, was a standard triaxial loading, but the loading was stopped at various points and allowed to creep for approximately 4 min and then the load was increased. Several of the tests used a combination of these load types. All tests were loaded into the post peak regime.

The displacement was manually controlled except for the uniaxial tests performed on the Instron 1323, which were electronically controlled. The rate of deformation was between 0.13 and 0.25 mm/min for the tests. The rates varied from test to test slightly and during each test. Except for the tests noted below, most test rates were close to the range mentioned above.

Specimen 1.21 was rapidly 'shock' loaded due to a problem with the universal testing machine's control unit. The displacement rate was increased threefold at about 90% of the peak load in the pre-peak regime and continued into the post- peak regime for sample 2.23. The displacement rate was increased from 20-fold at the peak load for 15 s for 2.17 and 2.21. The displacement rate was increased 5-fold at the peak load 45 s for 4.7. The displacement rate was increased in the post-peak regime three to ten for specimens 2.18 and 2.14. The displacement rate was slowly and continuously increased during the loading from 0.13 mm/min to greater than 0.63 mm/min at the peak load for samples 3.23, 3.24 and 3.25. The displacement rate for sample 3.8 was greater than 0.51 mm/min throughout most of the test.

RESULTS FAILURE ORIENTATION

Figure 2 shows the relationship between the measured angles and the confining pressure for the cylindrical specimens. Figure 2 shows a definite trend of a change in the angle with increasing confining pressure. This result compares well with the results obtained by Wawersik and Brace[1] shown in Fig. 3. Angles are measured from the direction of the maximum compressive load.

Some out-liers are noted in Fig. 2. Sample 1.21 was rapidly loaded when the control of the Tinius Olson Super 'L' malfunctioned. The displacement rate for samples 2.17, 2.21 and 2.18 was increased before or near the peak stress. The load rate was not changed for sample 4.17, however, this sample was relaxed in the post-peak, i.e. the displacement was held constant while the load decreased. The failure surface for 4.17 is a vertical split with a cone on one end. The load–displacement curve for 4.17 is 'jumpy' in the post-peak regime just prior to the relaxation. It is unknown if the behavior was due to some possible irregularities in the cap/sample interface or the relaxation process. The other out-liers did not have any special circumstance noted during the loading that might account for their deviation from the general trend.

FRICTION RELIEF

Rice[8] notes that the bifurcations associated with the loss of positive definiteness of the second-order work are sensitive to the assumed

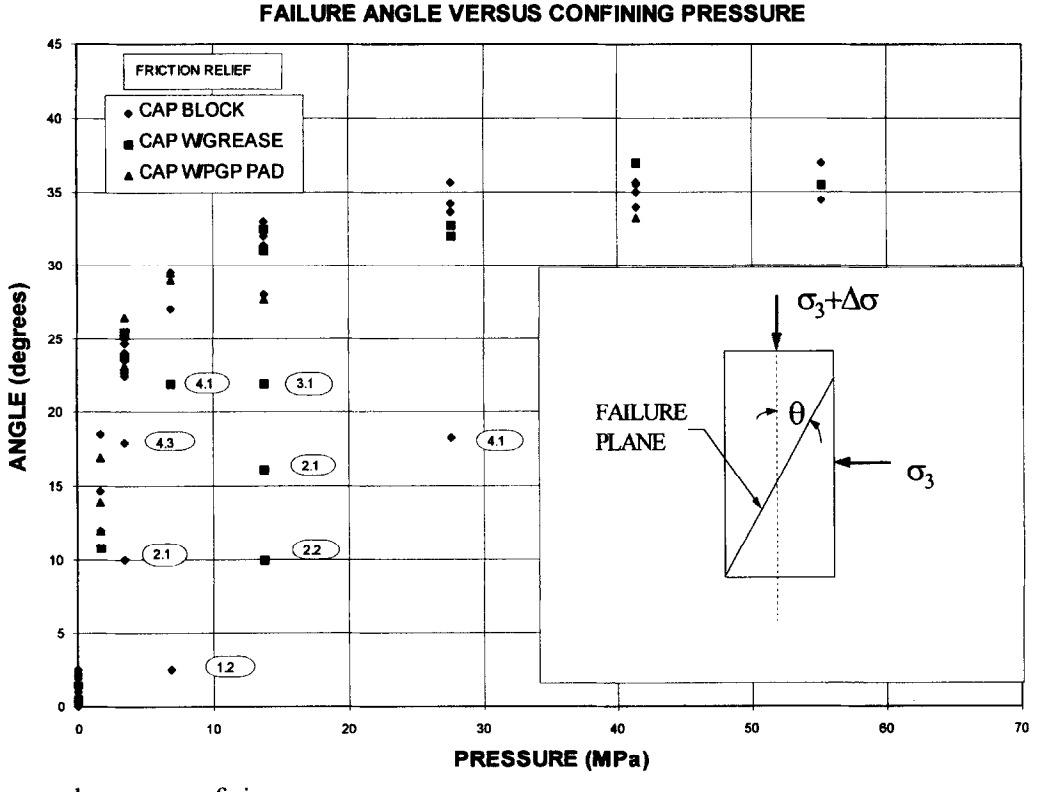

Fig. 2. Failure angle versus confining pressure.

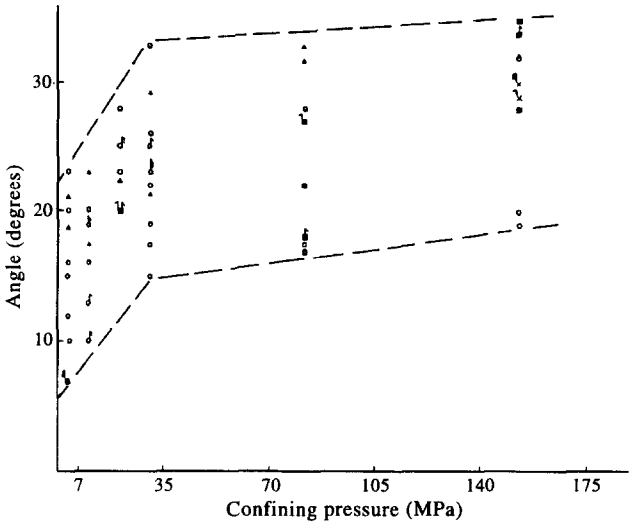

Fig. 3. Failure angle versus confining pressure for rock.

boundary conditions. Therefore, it is important to know how well an assumed state of stress is being simulated. The use of cap blocks with PGP pads did relieve friction to a negligible level as evidenced by the slipping of the specimens from between the cap blocks. The slipping was large at 14 and 28 MPa (2 and 4 ksi). The use of cap blocks with grease did not cause slipping; however, the resulting failure under uniaxial stress produced vertical failures similar to the ones produced using the cap blocks with PGP pads and those obtained using rubber sheets, indicating adequate relief of the friction.

The use of cap blocks alone provided some relief; however, failure surfaces from these tests were more complex with some parts of the surface straight and flat while other parts were curved and cone shaped. Furthermore, use of cap blocks alone produced slight bulging and more surface cracks. These additional cracks caused the foil surface of the gauges to 'crinkle' much like tin foil that is crunched into a ball and then unraveled.

From the X-ray tests presented by Rutland[9] it is shown that the direct contact of specimen and platen will produce friction between the platen and specimen that will confine the ends of the specimen causing a densification of the sample above that would occur under true uniaxial conditions. Furthermore, these tests indicate that the use of rubber sheets to relieve the friction tend to induce tensile forces in the specimen causing it to dilate much sooner than it would under true uniaxial conditions. Therefore, to obtain a true state of uniaxial stress in the specimen, the relief of the friction must be by a means that lies somewhere between no relief and rubber.

One indicator of the relief of the friction is the shape/location of the failure plane near the ends of the specimen. For uniaxial tests with no relief of the end friction, the failure surface would skirt the edge of the specimen end, but would not have any cracking across the end (Fig. 4(a). The failure produces a spoon or shoehorn-shaped surface with a corresponding cone shape on the other side (Fig. 4b). Uniaxial tests using PGP pads gave mixed results with cracks on one end oriented straight across the end of the specimen while cracks on the other end went around the edges (Fig. 5(a,b)).

Uniaxial tests using cap blocks alone for relief produced cracks that were straight across the end and a few cracks that followed the edge of the specimen. However, the collection of several cracks on the ends produces a failure with complex flat and curved surfaces (Fig. 6(a,b)). Uniaxial tests using caps with grease produced failures with cracks that run straight or nearly straight across the ends of the sample (Fig. 7(a,b)). Failures often produced three pie-shaped pieces, when viewed from the ends, with the angle between the cracks approximately 120° apart. For the samples that used PGP pads with cap blocks, the cracks were essentially straight from crack tip to crack tip across the end of the specimens. Furthermore, these samples needed the placement of a hose clamp at the interface of the cap and the specimen because the specimen kept slipping out from between the cap blocks. This slippage continued even with the clamps intact during the triaxial tests (Fig. 8). This slippage is further evidence of friction relief. When rubber was used in uniaxial tests to relieve end friction, the cracks transcended the ends and were straight from one crack tip to the other (Fig. 9(a,b)).

LOCALIZATION

Localization begins when non-homogeneous deformations occur in a uniformly loaded homogeneous material. For the purposes of this study, it is assumed that the friction on the ends of the specimens has been relieved sufficiently to consider the specimens homogeneously loaded. However, the results of the tests indicate that this is probably not true for tests with

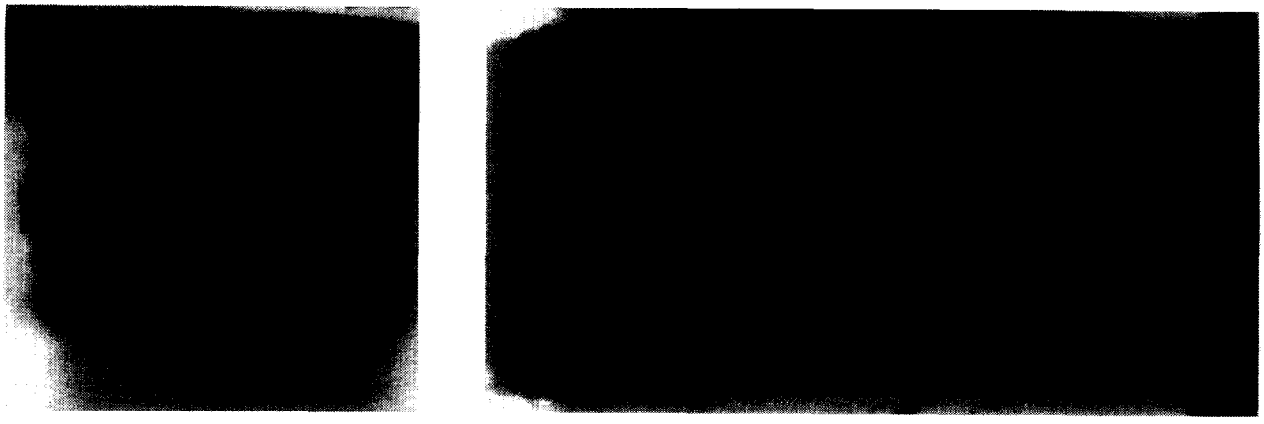

(a) 3.2 (b) 3.2 Side View

Fig. 4. Specimens with no friction relief.

cap blocks alone. It is further assumed that load variations due to the imperfections, camber and slope, in the cap/specimen interface are negligible.

One indicator of localized behavior is the presence of one or two failure planes while there is a conspicuous lack of cracking or failure plane development elsewhere in the specimen. Figure 10 shows the existence of such planes. Tests using cap blocks alone for friction relief resulted in numerous 'slip' surfaces, which were evident on the samples particularly at high confining pressures. Numerous 'slip' surfaces are evident in pictures of samples tested by Chinn and Zimmerman[10] who provided no relief to the end friction. Figure 11 shows some

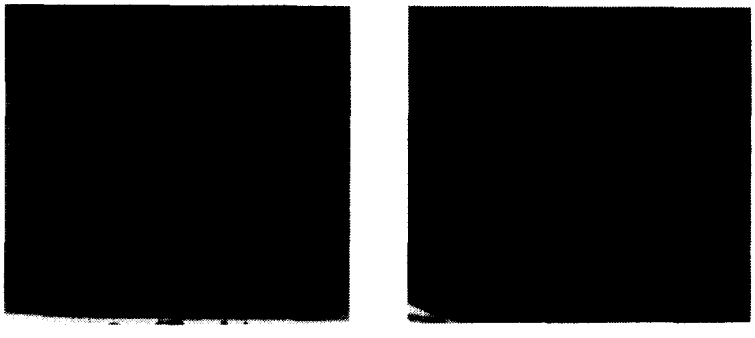

(a) 4.10 (b) 4.10

Fig. 5. Specimens using PGP pads for friction relief.

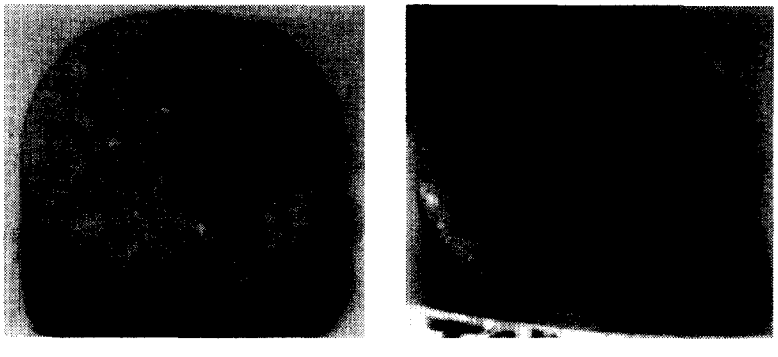

(a) 1.16 (b) 2.8

Fig. 6. Specimens using cap blocks for friction relief.

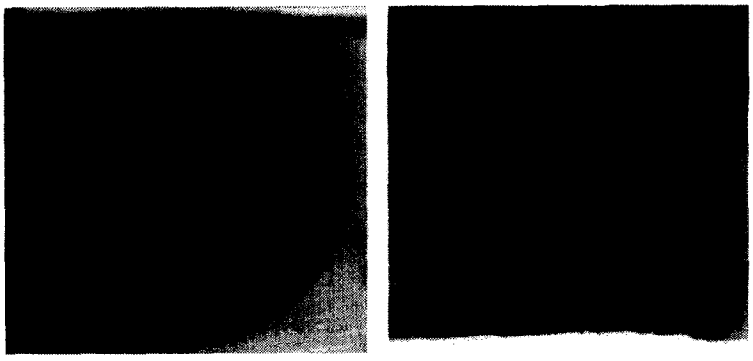

(a) 4.14 (b) 4.16

Fig. 7. Specimens using cap blocks and grease for friction relief.

samples from this report. The number and magnitude of these 'slip' planes are far greater than those found in the tests in this study, but are similar to those observed. The barrel shape of the specimens is very pronounced. From Fig. 11 it is easy to see why some may have interpreted the failure as a diffuse failure.

A second indicator of localized behavior is the reduction of strain in one or more of the strain gauges under increasing displacement. The point at which this occurs is an indicator of when in the loading process localization occurs. Figure 12 shows a plot of the strain from the strain gauges vs the displacement strain. At point A the displacement strain is increasing,

Fig. 8. Specimens using cap blocks with PGP pads for friction relief (3.24).

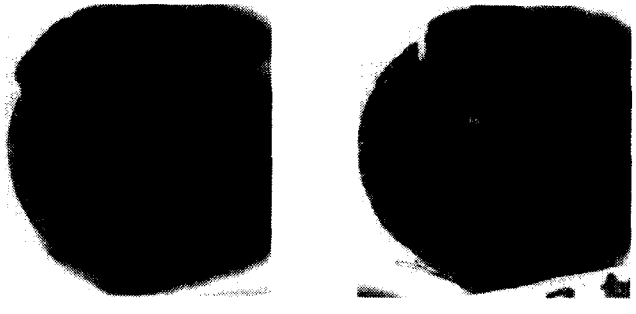

(a) 3.4 (b) 3.4

Fig. 9. Specimens using rubber sheets for friction relief.

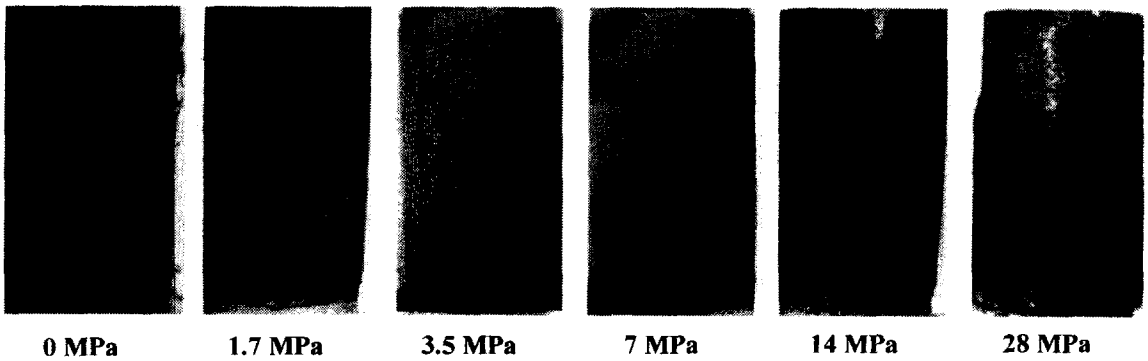

0 MPa 1.7 MPa 3.5 MPa 7 MPa 14 MPa 28 MPa

Fig. 10. Specimen failures at various pressures.

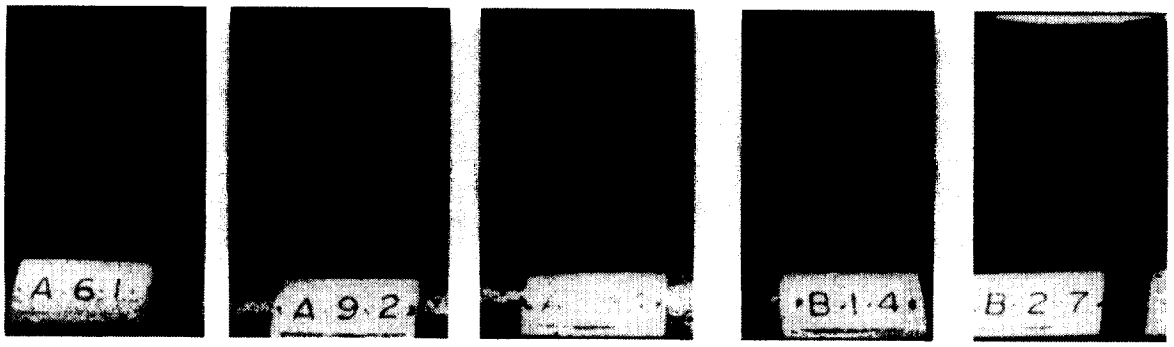

Fig. 11. Triaxial test samples w/No friction relief.

point A the displacement strain is increasing, while the strain from the strain gauge is decreasing, thus, localized deformations have occurred within the specimen. Comparing point A with the load–displacement curve indicates that this localized behavior occurred at the peak load. Analysis of the data from all of the tests shows that localized deformation begin within 5% of the peak stress in the pre-peak regime regardless of the confining pressure.

For uniaxial tests not conducted inside the triaxial cell, cracks/failure planes were detected by sound and with the naked eye at within 2% of the peak load. Dunn *et al.*[11] and Wawersik and Fairhurst[12] report that visible cracking did not appear until after the peak load.

MOHR ENVELOPE

The strength data was averaged to produce a single graph shown in Fig. 13. In addition to the Mohr circles, a line (radius) was added to each circle at an angle of 2ϕ, where ϕ depicts the average of the measured angle of the failure plane for each pressure. Two additional lines, radii, were added to each circle at angles of $2\phi - 5°$ and $2\phi + 5°$ to provide for a possible error, $\pm 2.5°$, in the measure of the failure angle. An error of $\pm 1.5°$ was used for the uniaxial circle.

A tangent was drawn from the 56 MPa (8 ksi) circle to the 3.5 MPa (.5 ksi) circle. The envelope is tangent to the 3.5–56 MPa circles.

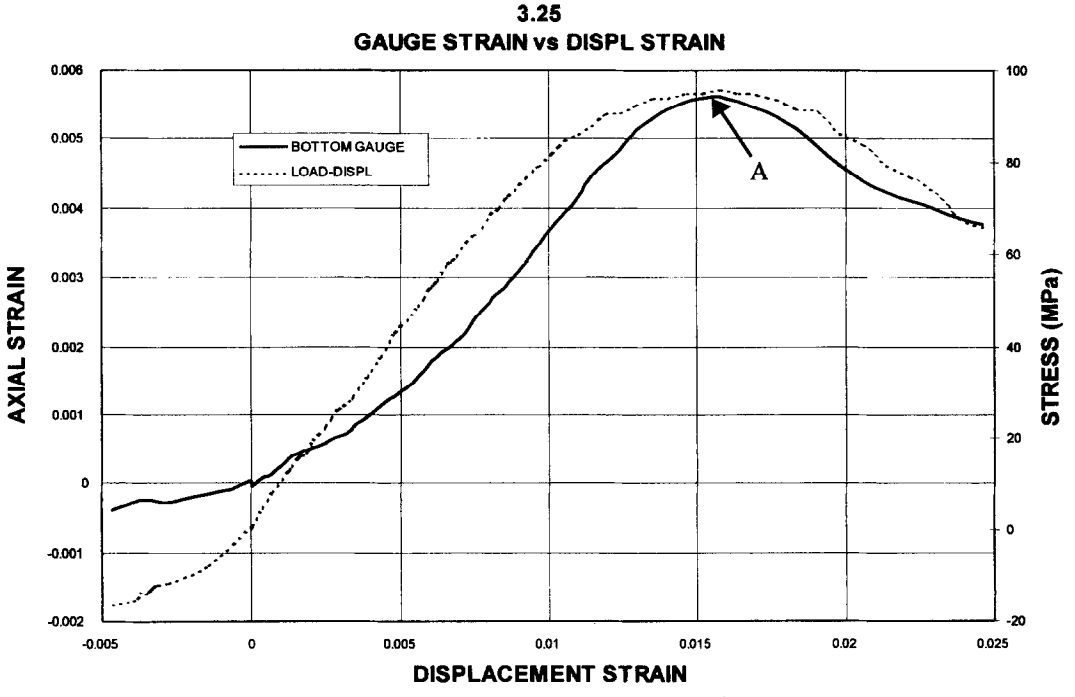

Fig. 12. Localization from axial gauge strain versus displacement strain (3.25).

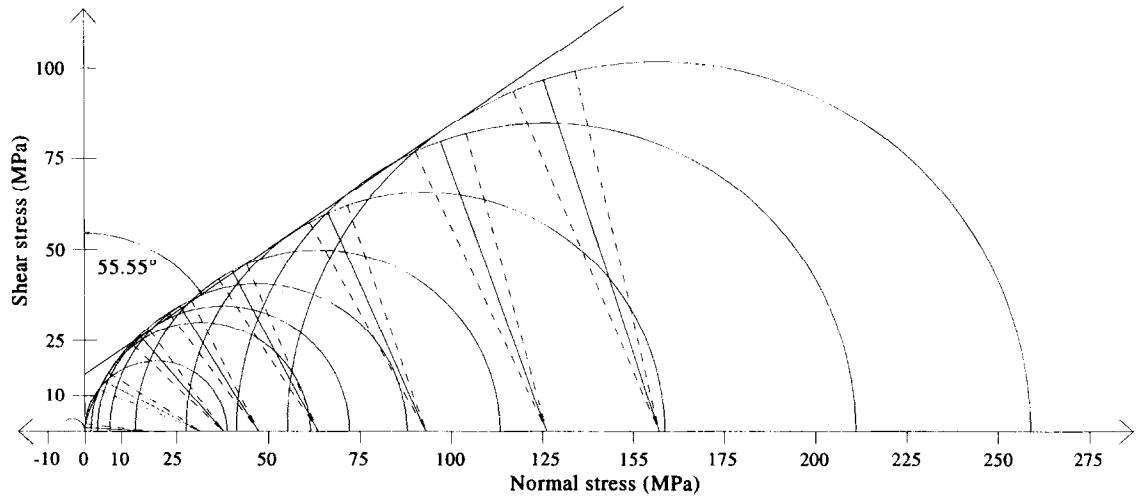

Fig. 13. Average Mohr circlesfor triaxial test series.

However, it is not very close to the 1.7 MPa (0.25 ksi), 0 MPa and tensile circles. Further examination of Fig. 13 shows that the angle predicted by the envelope does not accurately reflect the measured angles at low and high pressures. Thus, the use of the Mohr envelope as a damage or plasticity surface in the classical manner is not applicable to the tests in this study, except in the median pressure region from 3.5 to 28 MPa. Furthermore, the use of a classical Mohr envelope fails to predict the dependence of the strength (maximum stress) on the intermediate principle stress.

MAXIMUM AXIAL STRESS VS CONFINING PRESSURE

Figure 14 shows the maximum axial stress vs confining pressure. Several out-liers are noted.

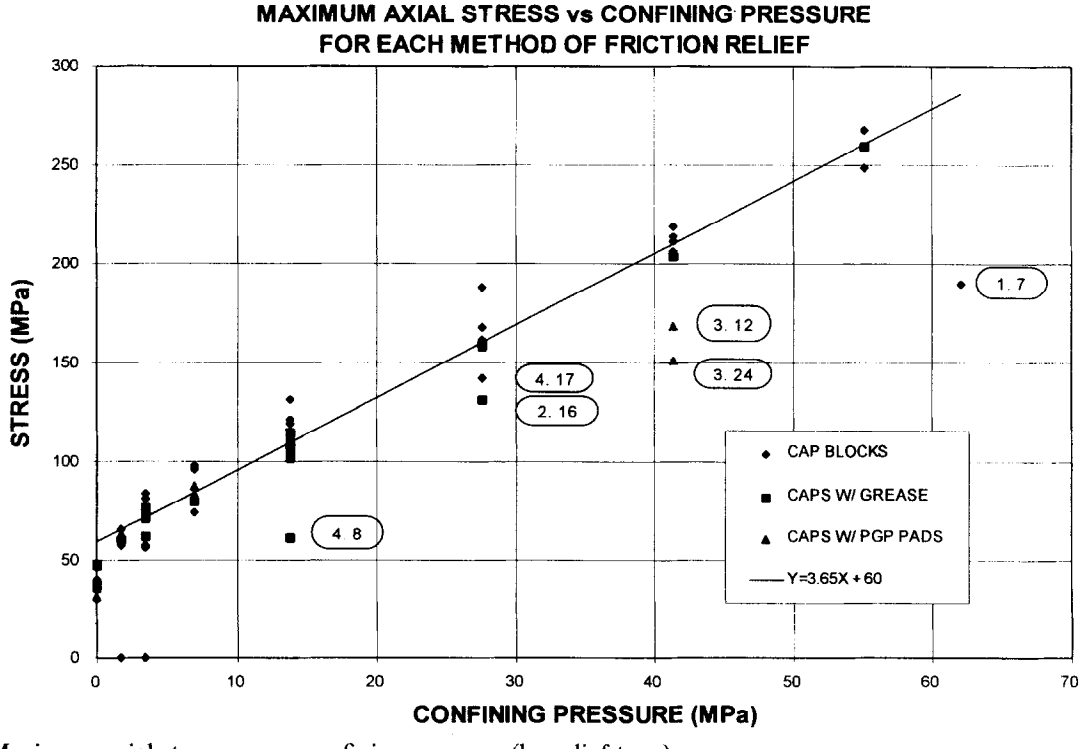

Fig. 14. Maximum axial stress versus confining pressure (by relief type).

Specimen 4.08 was damaged during preparation. Specimens 3.24 and 3.12 slipped during testing. During the testing of specimen 1.07 the cap block failed, but the sample did not. A line was fit to all of the data except the uniaxial data and the out-liers.

OCTAHEDRAL SHEAR VS OCTAHEDRAL NORMAL

Figure 15 shows the octahedral shear vs the octahedral normal stress. The line A–A represents the states of equal shear and normal stress. Comparing this data with Fig. 2, angle vs confining pressure, the slope of the orientation vs confining pressure is large up to about 14 MPa. The slope decreases dramatically at 14 MPa. All tests at pressures lower than 14 MPa have peak octahedral shear stresses greater than their corresponding peak octahedral normal stresses. All tests at pressures greater than 14 MPa have peak octahedral shear stresses less than their corresponding octahedral normal stress, while tests at 14 MPa are at the point of equal peak octahedral shear and normal stresses. This correlation between the ratio of octahedral shear and normal stresses and the rate of change of the failure orientation with increasing confinement indicates an influence of the ratio of the peak octahedral shear to octahedral normal on the failure mechanism.

DISCUSSION

In this study a change in the angle of the failure plane was observed as the confinement on the sample increased. Zimmerman and Traina[5] state 'Failure appears to be by expansion in the direction of the minimum principal stress.' Platens were used to apply the lateral loads which were constrained from allowing failure (localization) in any direction other than parallel to the maximum compressive stress. This explanation of deviation from the results of this study are corroborated by the results of Gerstle *et al.*,[6] who have found that boundary constraints inhibit transverse deformations.

When no effort is made to relieve the friction between the samples and the axial load application, the samples will take on a barrel shape similar to the samples shown in Fig. 11. The lack of friction relief leads to the development of conical regions near the ends that are compressed more than the rest of the sample. The cones act as wedges driving the material in the center out laterally.

From Fig. 2 the change in orientation with increasing confining pressure may be inter-

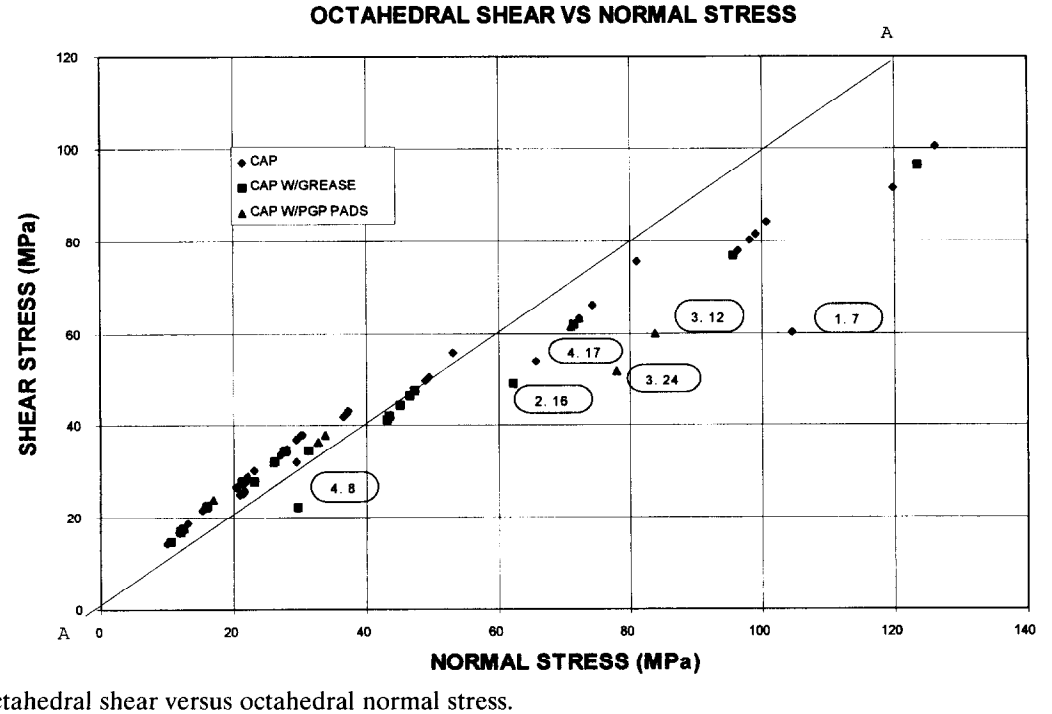

Fig. 15. Octahedral shear versus octahedral normal stress.

preted as a change in mode from a vertical splitting to an angled shear failure with a transition from one mode to the other between 0 and 7 MPa. Furthermore, this may be considered as evidence of two separate limit surfaces. Rutland[9] shows that the change in orientation of the failure plane can be predicted with a single limit surface.

PLASTIC DEFORMATIONS

The data for uniaxial tests and tests at 1.7 MPa show large plastic lateral deformation in comparison to the axial plastic deformations. As the confining pressure increases, the majority of the plastic deformation is in the axial not lateral direction. Tests at 42 MPa produced axial plastic strains 5 to 10 times larger than the lateral plastic strains. At 3.5 MPa the axial plastic strain is about three times larger than the lateral plastic strain. The amount of lateral strain compared to axial strain increases during the loading process.

DAMAGE

Classical damage mechanics (CDM) focuses on changes to the moduli. Most models consider changes to the bulk modulus, K, and the shear modulus, G. Therefore, the changes in these material properties were investigated by examining the changes to the axial (sometimes referred to as Young's) modulus, E, and the lateral extension ratio, ν.

The initial modulus and lateral extension ratio were 31 GPa (4500 ksi) and 0.21, respectively, for tests with friction relief. This yields bulk and shear moduli of 18 GPa (2600 ksi) and 13 GPa (1900 ksi), respectively. The initial modulus and lateral extension ratio begin to degrade at about 60% of the peak stress. The modulus degrades to approximately 85% of the initial value while the elastic lateral extension ratio increases to approximately 120% of the initial value. Thus, the bulk modulus at the peak stress is equal to the initial bulk modulus and the shear modulus reduces by approximately 25% to 10 GPa (1500 ksi). This result is consistent with generally accepted results and numerous damage models.

CONCLUSIONS

While these conclusions are definitive for the material studied here, it is surmised that these conclusions apply universally to all cementitious materials, however, further study is required to confirm this.

The angle of the failure plane relative to the direction of maximum compressive stress increases with increasing confining pressure.

The failure is characterized by a discontinuous bifurcation (a zone of localized deformation develops). Localized deformations occur within 5% of the peak stress in the pre-peak regime.

Use of platens to apply lateral pressure constrain possible failure modes.

Constraint due to end friction will influence the resulting failure. Use of cap blocks alone is insufficient to relieve end friction and may cause cones to form near the ends.

The behavior of the sample that was 'shocked' and those that were tested at higher strain rates suggest that the angle of the failure plane relative to the direction of maximum compressive stress decreases with increasing strain rate. While the results of these tests are by no mean conclusive with regard to this relationship, the possible correlation between strain rate and the orientation or mode of faliure is worthy of note and further research.

ACKNOWLEDGEMENTS

The authors wish to gratefully acknowledge the partial support of the National Science Foundation. Dr Ken P. Chong is the program manager.

REFERENCES

1. Wawersik, W. R. & Brace, W. F., Post-failure behavior of a granite and diabase. *Rock Mechanics*, **3** (1971) 61–85.
2. Murrell, S. A., The effect of triaxial stress systems on the strength of rocks at atmospheric temperatures. *Geophysics Journal of the Royal Astronomical Society*, **10** (1965) 231–281.
3. Palaniswamy, R. & Shah, S. P., Fracture and stress–strain relationship of concrete under triaxial compression. *Journal of the Structures Division, ASCE*, **ST5** (1974) 901–916.
4. Palaniswamy, R. and Shah, S. P., Deformation and failure of hardened cement paste subjected to multi-

axial stresses. *Proceedings of the RILEM International Symposium: The Deformations and the Rupture of Solids Subjected to Multiaxial Stresses*, 1972, pp. 169–179.
5. Zimmerman, R. M. & Traina, L. A., Strength and deformation response of concrete under multiaxial loadings — cooperative project. Final report ENG 74-12097 for National Science Foundation, 1977.
6. Gerstle, K. H., Linse, D. L., Bertacchi, P., Kotsovos, M. D., Ko, H. Y., Newman, J. B., Rossi, P., Schickert, G., Taylor, M. A., Traina, L. A., Zimmerman, R. M. & Bellotti, R., Behavior of concrete under multiaxial stress states. *Journal of the Engineering Mechanics Division ASCE*, **0** (1980) 1383–1403.
7. Labuz, J. F. & Bridell, J. M., Reducing frictional constraint in compression testing through lubrication. *Experimental Mechanics*, **0** (1991) 0 (submitted)
8. Rice, J. R., The localization of plastic deformation. theoretical and applied mechanics. *14th IUTAM Congress*, ed. W. T. Koiter. North-Holland, 1976, pp. 207–220.
9. Rutland, C. A., Effects of confinement on the failure mechanism in cementitious materials. Ph.D. dissertation, University of New Mexico, Albuquerque, NM, 1995.
10. Chinn, J. & Zimmerman, R. M., Behavior of Plain Concrete Under Various High Triaxial Compression Loading Conditions. Air Force Weapons Laboratory Technical Report no. AFWLTR 64-163, 10 May 1965.
11. Dunn, D. E., LaFountain, L. J. & Jackson, R. E., Porosity dependence and mechanism of brittle fracture in sandstones. *Journal of Geophysical Research*, **78** 14 (1973) 2403–2417.
12. Wawersik, W. R. & Fairhurst, C., A study of brittle rock fracture in laboratory compression experiments. *International Journal of Rock Mechanics and Mineral Science*, **7** (1970) 561–575.